

**LOW CYCLE FATIGUE ANALYSIS OF FRICTION STIR WELDED AND
TIG WELDED AL-MG-SI ALLOY SIMILAR JOINTS**Akshansh Mishraa¹, Anish Dasgupta²^{1,2} Department of Mechanical Engineering, SRM Institute of Science and Technology, Kattangulathur

Abstract: In this study, Al-Mg-Si alloy plates in 4 mm thickness that are particularly used for aerospace and automotive industries were welded using Tungsten Inert Gas (TIG) welding and Friction Stir Welding (FSW) methods as similar joints with one side pass with parameters of varying tool rotation, weld speed and 2.3 degree tool tilt angle. Tensile tests results showed high yield stress values for FSW joints. Micro Vickers hardness test gave the required result for FSW welded and TIG welded Al-Mg-Si alloy plates. While fatigue test results showed all similar welded joints have fatigue strength close to each other.

Keywords: Weld Zones; Friction stir welding; Metallurgical Test; Mechanical Test; Fatigue Analysis

1. Introduction

Friction Stir Welding is a solid state joining process developed in 1990 and is nowadays frequently used to join aluminium alloys. The FSW process is fast and it can be automated easily. This results decrease in manufacturing cost and production time. Low weight, good weldability and good mechanical properties make aluminium alloys commonly used engineering materials. However, it was found that aluminium was difficult to weld with conventional fusion welding process due to formation of intermetallic compounds between the joints which results in poor strength.

There are many factors that make the weld critical under fatigue loading conditions. For instance, stress concentrations such as weld toe and weld root, residual stresses, unfavourable mechanical properties of the weld nugget and potential defects in the weld are major causes of weld failure in service. Weld failure leads to loss of lives and substantial costs each year all over the world. Fatigue analysis helps to identify how repetitive load cycles cause structural failures. In transportation and under varying load conditions fatigue failure is an important issue. It helps us to identify failures in components subjected to stress less than yield and do not experience plastic deformation and have relatively long lives.

M. Czechowski *et al.*, (2005) successfully welded alloys EN-AW 5058 H321 and EN-AW 5059 H321 (Alustar) were welded by FSW (friction stir welding) method. The FSW welds showed better properties in comparison to the joints welded by the MIG method. The test of microstructure proved the proper structure of the weld which consisted of following: welded nugget, thermo-mechanically affected zone (TMAZ), heat affected zone (HAZ) and unaffected material. D.R. Ni *et al.*, (2014) carried out FSW process on a semi-solid processed (thixomolded) Mg-9Al-1Zn magnesium alloy (AZ91D), aiming at evaluating the weldability and fatigue property of the FSW joint. Microstructure analysis showed that a recrystallized fine-grained microstructure was generated in the nugget zone (NZ) after FSW. The yield strength, ultimate tensile strength, and elongation of the FSW joint were obtained to be 192 MPa, 245 MPa, and 7.6%, respectively. Low-cycle fatigue tests showed that the FSW joint had a fatigue life fairly close to that of the BM, which could be well described by the Basquin and Coffin-Manson equations. Michael Besel *et al.*, (2015) studied the effect of Friction Stir Welding on the fatigue behaviour of Al-Mg-Sc. To reveal the influence of the welding parameters, different travel speeds of the welding tool have been used to provide weld seams with varying microstructural features. Crack initiation as well as crack propagation behaviour under fatigue loading has been investigated with respect to the local microstructure at the crack initiation sites and along the crack path.

This paper deals with the mechanical and fatigue analysis of welded joints made by the Friction Stir welding process and Tungsten Inert Gas (TIG) Welding process. Previous studies indicate that the fatigue properties of TIG welds differs from those of conventionally welded. Due to this level of fatigue strength and also the slope of S-N curves for FSW is different compared to existing fatigue design standards for arc-welding. We have welded similar plates of dimensions 150mm×100mm×4mm of AA6061-T6 aluminium alloy.

2. Experimental Procedure

In this study, 6061-T6 aluminium alloys were used as base metals. Aluminium alloy plates were machined to required dimensions for butt welding. For Friction Stir Welding H13 tool steel with chemical composition 0.406% C, 1.096% Si, 0.443% Mn, 4.952% Cr, 1.251% Mo, 0.183% V with given dimensions was used as weld tool as shown in Fig.1. Varying welding parameters like tool rotation speed, welding speed and feed depth were used as shown in Table 1. Similar joints of 6061 aluminium alloys were fabricated using these parameters. While during TIG welding, the

parameters used for welding similar joints 6061-6061 aluminium alloys, power source was AC at a frequency of 50 Hz with current and voltage value of 1600A and 40V. The filler material used in TIG welding was ER-4043. This filler material is Silica rich compound which inhibits the formation of intermetallic compounds which results in poor weld quality. These specimens were used for micro hardness assessment under 100g load after microstructure test. For fatigue test, standard specimen was prepared as shown in Fig. 2. The specimen was subjected to low cycle fatigue test.

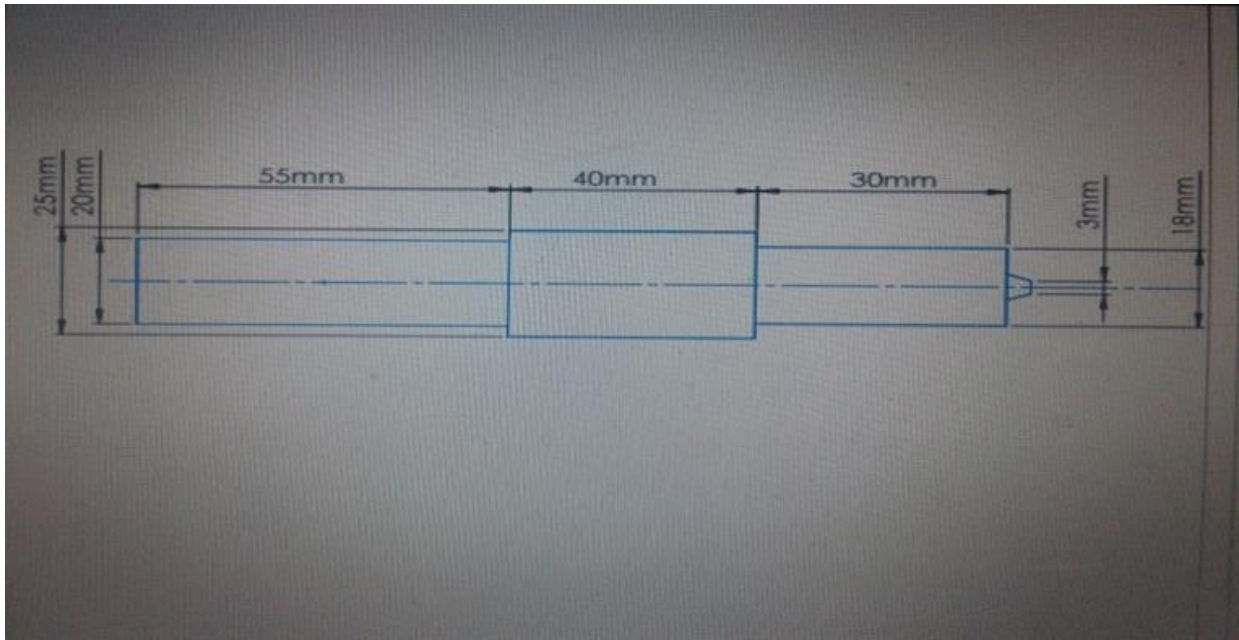


Figure 1: Tool design of H13 Tool steel

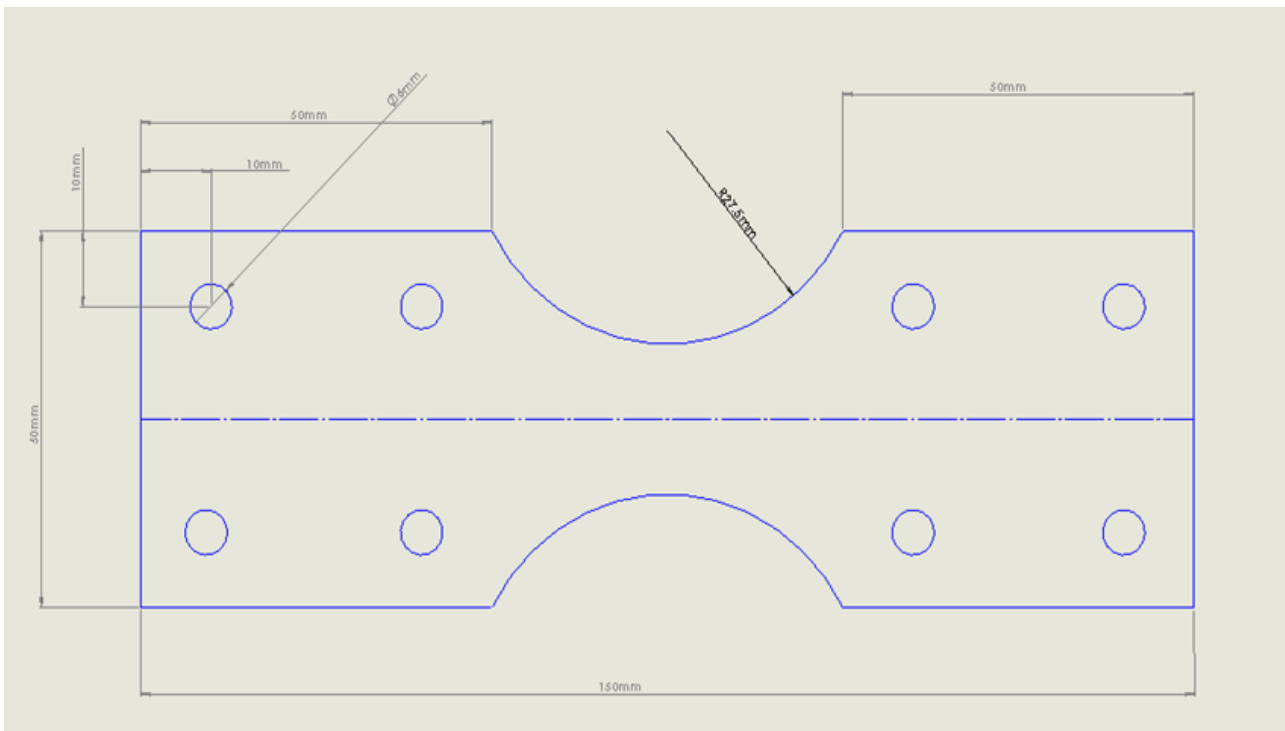


Figure 2: Design of Low cycle fatigue test specimen

3. Results and Discussions

3.1 Micro hardness Testing

The Vickers hardness test method is based on an optical measurement system. The Micro hardness test procedure, ASTM E-384, specifies a range of light loads using a diamond indenter to make an indentation which is measured and converted to a hardness value. The data for micro hardness were obtained with 100gm load. A square base pyramid shaped diamond is used for testing in the Vickers scale. The hardness value for FSW is given in the form of graph as shown in Fig.3. The hardness value was taken from distance of every 2mm from weld joint.

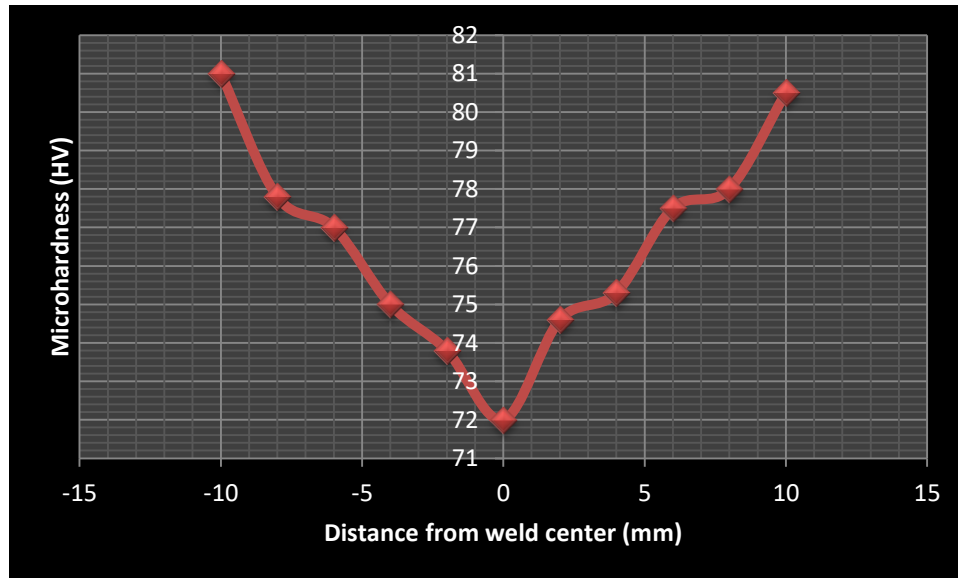


Figure 3: Micro hardness for FSW AA6061-T6 Joints

It is observed that Base metal zone has more hardness value while Nugget zone has less hardness value compared to TMAZ and HAZ. According to Hall-Petch equation the hardness in Nugget zone should be higher but the main reason for its less hardness is melting of precipitates due to supply of heat. It is also observed that the graph is not symmetrical. The main reason is improper flow of material during joining process. Micro hardness of TIG Welded joint is tabulated in Table 1.

Table 1: Micro hardness of TIG welded joint

Current (A)	Weld Zone(HV)	Fusion Zone(HV)	Heat Affected Zone(HV)
160	71.06	76.06	80.23

3.2 Tensile Testing

Tensile properties of both Friction Stir Welded and TIG welded joints are given in Table 2. Tensile test results for FSW joints were above values results has been obtained from previous studies. It was observed that the failure occurs at the zone which has less hardness i.e. in the weld zone. This was due to majority strength loss in weldments in strain-hardened due to the recrystallization process.

Table 2: Tensile test analysis of FSW and TIG Welded joints

Type of Joint	Area mm ²	Ultimate Load (KN)	Gauge Length (mm)	UTS(MPa)	%Elongation
FSW	58.18	16.98	50	293	8.8
TIG	58.18	12.7	50	260	5.08

It is observed that the Friction Stir Welded joint has more yield stress compared to TIG welded joints. And also it is seen that Friction Stir Welded joint has more elongation than TIG welded joints.

3.3 Fatigue Testing

To obtain S-N curves, seven Friction Stir Welding specimens and eight TIG welding specimens were tested. Based on the fatigue strength assessment recommended by the IIW statistical analysis and processing of fatigue experimental data were performed.

When $N_f < 2 \times 10^6$, then S-N equation was expressed as
 $\text{Log } N_f = \text{Log } K - m \text{Log } (S_n(f(t)) - Z\sigma$

Where, N_f is the fatigue life in cycles, K is the empirical constant, m is the slope coefficient of the S-N curve, S_n is the nominal stress, $f(t)$ is the thickness reduction factor, Z is the number of standard deviations, and σ is the standard deviation of $\text{Log } N_f$.

Low Cycle Fatigue measurement assembly shown as shown in the Fig.4 consisted of DC motor 220 volt 4.5 amps PMDC motor with extended shaft at both ends, Flange attached to the motor with lever fixing holes @ 5 mm, 7.5 mm, 10 mm, 15 mm from the centre of the flange, Position sensor, Test sample fixing arrangement, Proximity sensor NPN type 3mm sensing gap, Anti-vibration mountings, Strain gauge, 2pin, 3pin & 4pin connectors.

Low cycle Fatigue measurement instrument as shown in the Fig. 5 consisted of Data Acquisition board with 4 line LCD display, Key board, PC interface software, USB cable, PICOSCOPE 2002 DAQ system. Input from Strain amplifier board Output via another USB cable to PC, Strain amplifier board, Proximity sense pulse control board, Position sense amplifier board, Power ON/OFF switch and 2pin, 3pin, 4pin connectors.

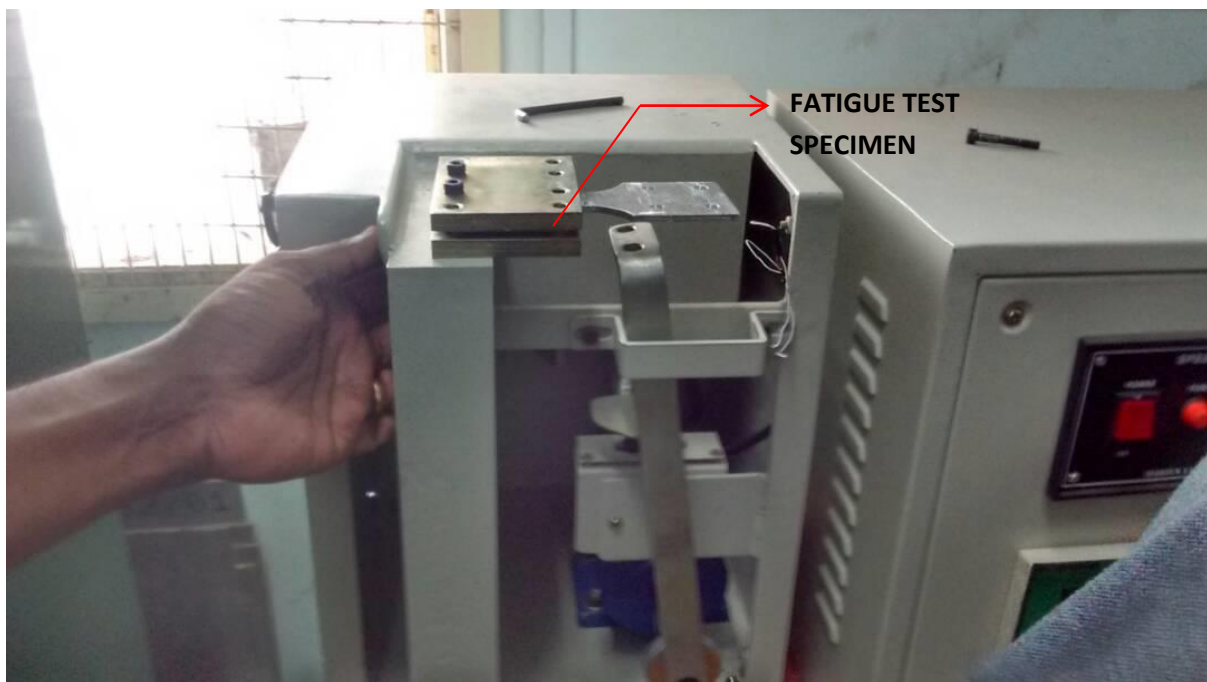


Figure 4: Low cycle Fatigue Measurement Assembly



Figure 5: Low cycle Fatigue Measurement Instrument

Software installed in the system for getting the reading of Fatigue testing were PICOSCOPE 2002 software, DAQ System software, Windows 8 software, PICOSCOPE 2002 guiding manual, Introduction to PC oscilloscope guiding manual, PICOSCOPE 2002 software CD and DAQ software CD.

The control panel and the Fatigue measurement control panel over the wooden table were assembled. Anti-vibration mounting for Fatigue measurement assembly was used. Both the Fatigue measurement assembly and the fatigue measurement instrument were interlinked by plug-in cables. The two pin connector from the strain sensor to strain amplifier board in the Fatigue measurement instrument was connected. The four pin displacement sensor connection cable was connected to the four pin male connector of the Fatigue measurement instrument. The three pin proximity sensor for speed measurement was connected to the three pin male connector of the instrument. Two pin power Connector cable of the PMDC motor was connected to the power connector of the speed controller. The contact NO-P from the fatigue measurement was connected to the drive speed controller for switching ON the Drive. A two pin connector was provided to regulate the speed of the motor. Two pin connector which provide 1-5 Volt Dc power to vary the speed of the motor should be connected to the motor driver.

The strain sensors shown in the Fig. 6 are used as a Fatigue Gauge. The fatigue gage is generally in the shape of a “dog bone” specimen as specified by American Standard Test Methods (ASTM) for testing tensile strength of a material. For example, a specimen may be 1/8 inch thick with a 2 inch Width on both ends and a 1/2 inch Width in the middle. Since the specimen looks like a “dog bone,” this term is used to refer to them. The specific geometry and dimensions of the fatigue gauge will depend on the application, i.e., a material of a uniform thickness and is made of the same alloy on which it is used to measure fatigue. The fatigue gauge is fixed directly to the surface of a metal or metal alloy component to be measured by means of an adhesive as shown in the Fig. 7. The adhesive may be, but without limitation, an epoxy, silicone, polyurethane. The adhesive is preferably coated on to one side of the gauge and is covered with a non-stick removable backing such as a foil or Teflon. Because the gauge experiences all the stresses of the component under measurement, it is as if the coupon test is being carried out in-situ. In other Words, the gauge may be described as a witness specimen. During the mounting of the gage is installed or mounted directly onto the surface of the component under measurement (the structural part being tested). Typically the gauge is mounted or installed close to the point of interest. As a crack is initiated in a gauge and it begins to grow, the cross sectional area of the gauge reduces. This reduction in area consequently increases the electric resistance of the gauge. The gauge may be connected to a controller that continuously or periodically measures and records resistance values of one or more fatigue gauges.

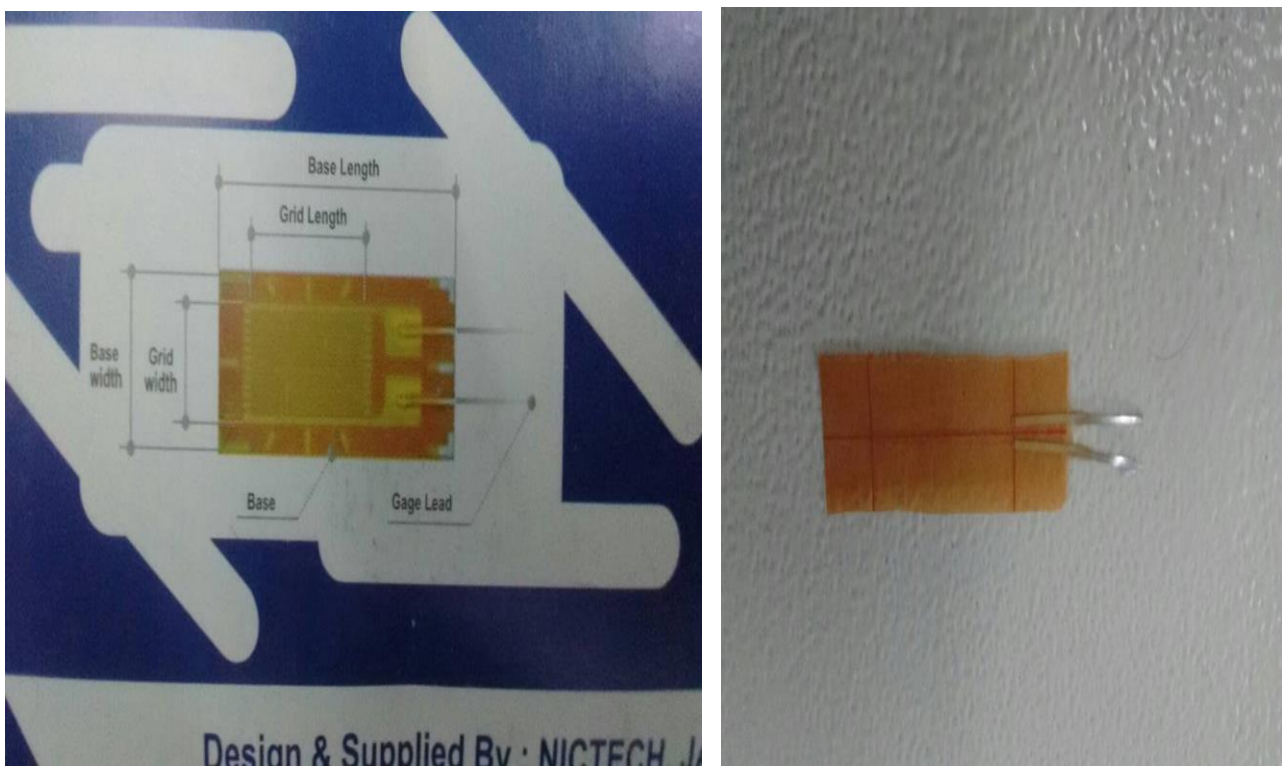


Figure 6: Fatigue Gauge used in Low Cycle Fatigue Testing

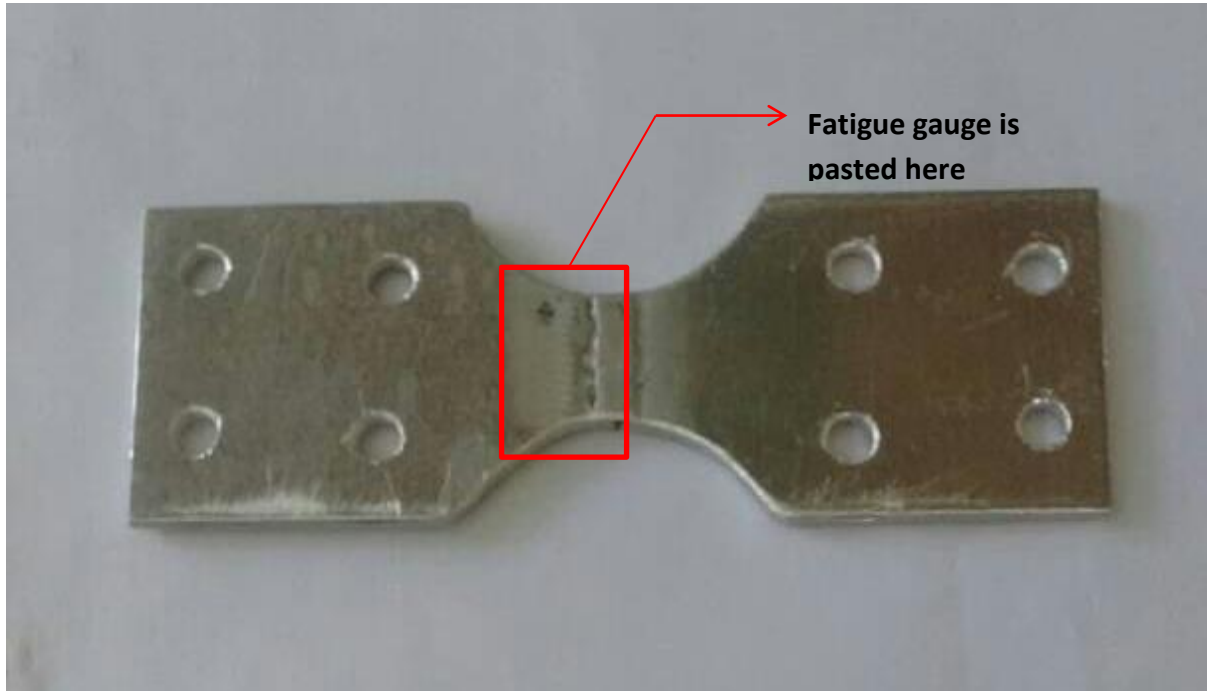


Figure 7: Position where Fatigue Gauge is pasted

An electric current is required only during inspection. A measuring-inspecting unit may supply the electric current and measure the resistance of the gage. In one of the embodiments, the measuring-inspecting unit supplies the 3 arms of a Wheatstone bridge while the 4th arm is the fatigue gage. When the gauge fails completely, there will be no current carried in the gage 100, and the structural part is in danger of failing due to fatigue. Fatigue gauges could be designed to resist constant amplitude fatigue cycles at stresses, such as 20 ksi, 30 ksi, 40 ksi, and so on, and tested to fail in the laboratory at 104, 105, and 106 cycles, for example. The gauge is a smooth dog-bone specimen. Gauges can also be designed to have stress concentrators or notches.

After pasting the Fatigue gauge on the welded joint, the specimen was mounted as shown in the Fig. 8. The power cord to a single phase mains supply was plugged in. The power to the equipment was Switched On. The data obtained are shown in the Table 3 for Friction Stir Welded joints and Table 4 for TIG Welded joints.

Table 3: Fatigue Analysis data of Friction Stir Welded joints

Frequency (HZ)	Motor Speed (rpm)	Movement (mm)	No. of cycle	Stress (MPa)
12.49	749	0.215	2609	136
12.87	773	0.217	3479	132
13.23	798	0.217	4063	127
13.81	829	0.223	4751	123
14.01	851	0.265	5628	119

Table 4: Fatigue Analysis of TIG Welded Joints

Frequency (HZ)	Motor Speed (rpm)	Movement (mm)	No. of cycle	Stress (MPa)
10.75	645	0.425	3364	125
11.11	666	0.427	3915	122
12.56	719	0.432	4582	116
13.72	785	0.444	5145	113
15.34	920	0.478	5936	109

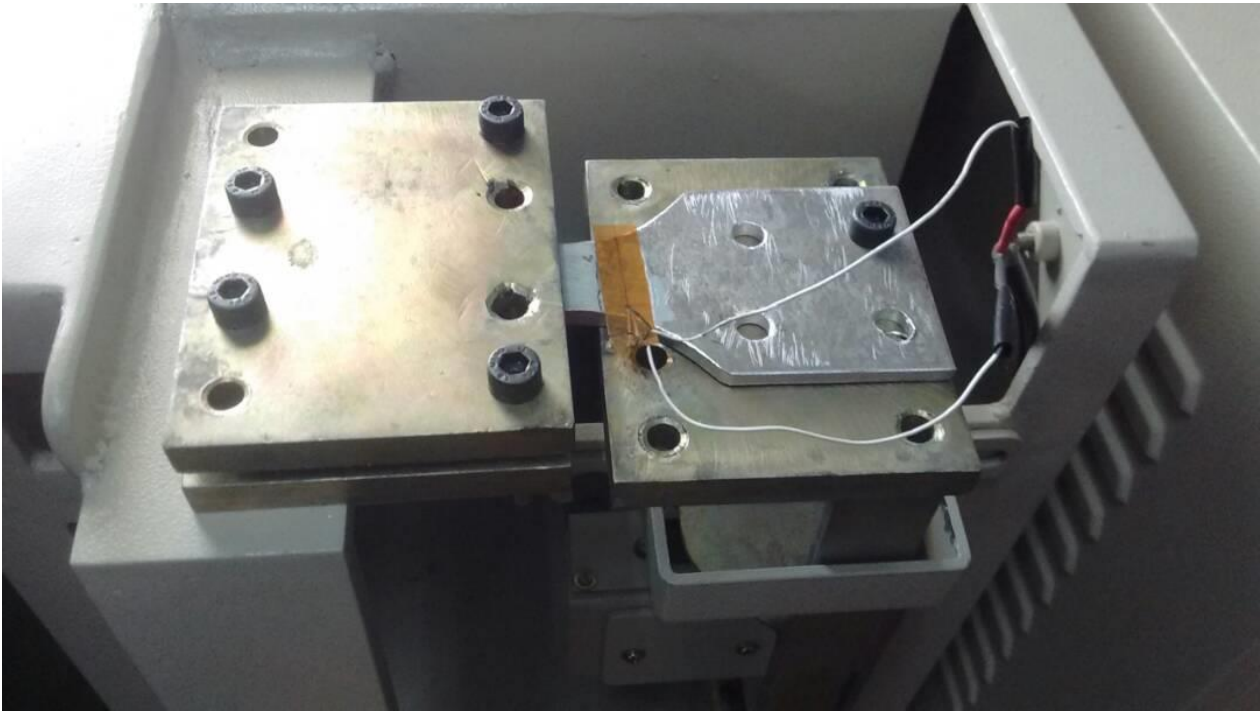


Figure 8: Fatigue test specimen mounted on Fatigue test assembly

The S-N curve plot and graph for Movement in mm plotted against Number of cycles of Friction Stir Welded Fatigue specimens are shown in the Fig. 9 and Fig. 10.

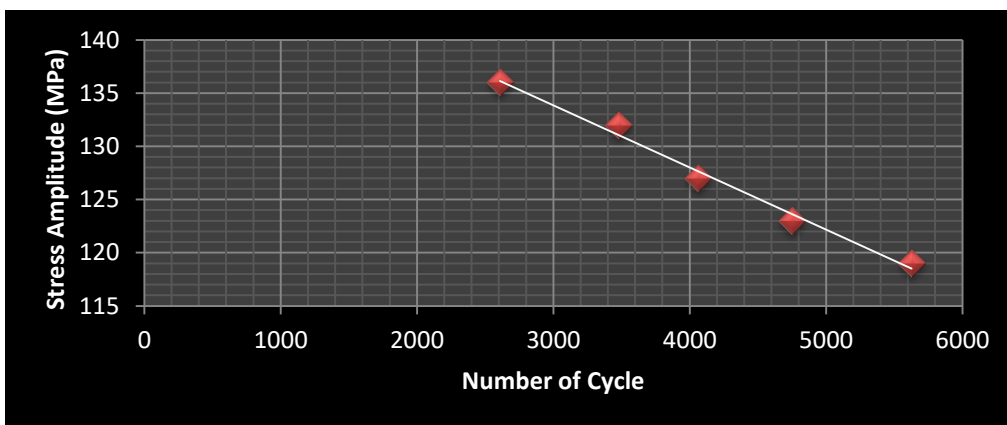


Figure 9: S-N curve for Friction Stir Welded Fatigue specimen

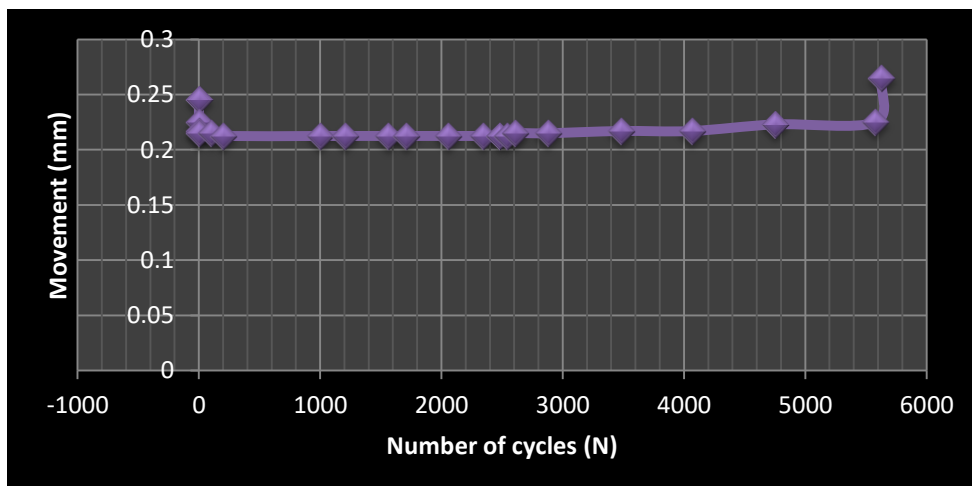


Figure 10: Movement (mm) vs. Number of cycles for Friction Stir Welded specimen

The S-N curve plot and graph for Movement in mm plotted against Number of cycles of TIG Welded Fatigue specimen are shown in the Fig. 11 and Fig. 10. The specimen after Fatigue testing is further shown in the Fig. 12.

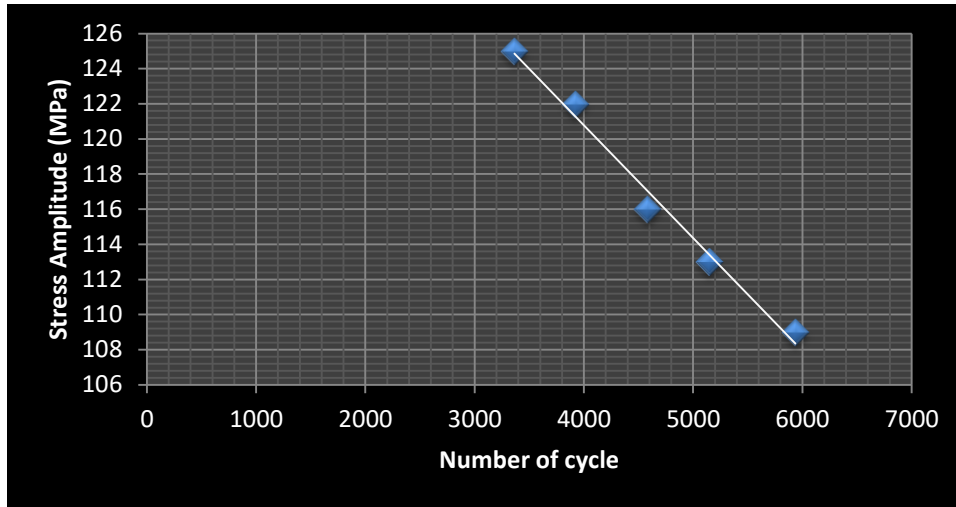


Figure 11: S-N Curve for TIG Welded Fatigue specimen

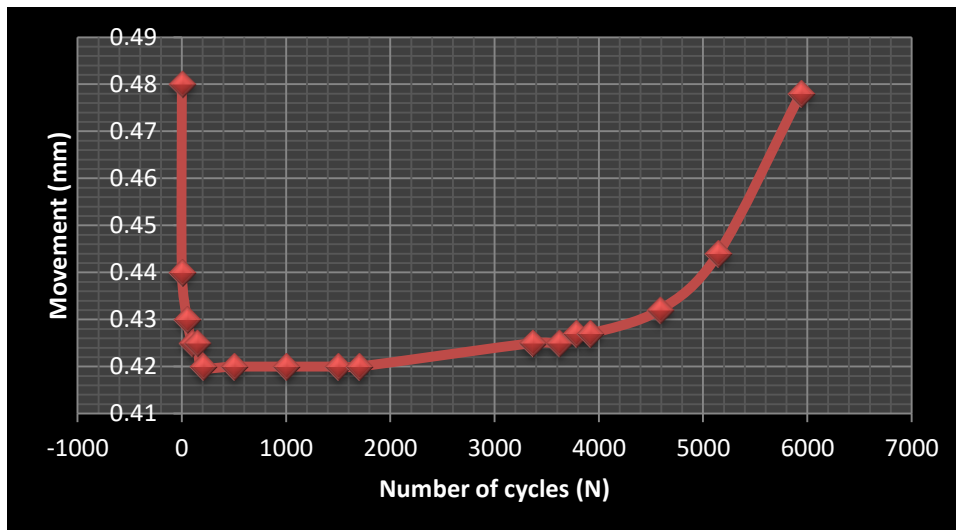


Figure 12: Movement (mm) vs. No. of cycles for TIG Welded Fatigue specimen



Figure 13: Specimen after Fatigue Failure

4. Conclusions

In this study, 4mm thick AA6061-T6 aluminium alloys that used widely in aerospace and automobiles industries were welded successfully using friction stir welding and TIG welding for similar alloy pair. Tensile test shows that FSW joints have higher strength and higher ductility compared to TIG joints. FSW has better strength than TIG welding process. Aluminium AA6061-T6 alloy welded by FSW method shows greater fatigue life in comparison to same alloy welded by TIG welding method. Fatigue failure was generally occurred in the zone among flow arm, weld nugget and Thermo Mechanically Affected Zone (TMAZ). Fatigue limits of all joint types were close to each other.

References

1. M. Czechowski (2005) 'Low-cycle fatigue of friction stir welded Al–Mg alloys' *Journal of Materials Processing Technology*, Vol.164-165, pp.1001-1006.
2. D.R. Ni, D.L. Chen, J. Yang, Z.Y. Ma (2014) 'Low cycle fatigue properties of friction stir welded joints of a semi-solid processed AZ91D magnesium alloy' *Journal of Materials and Design*, Vol.56, pp.1-8
3. Michael Besel, Yasuko Besel, Ulises Alfaro Mercado, Toshifumi Kakiuchi, Yoshihiko Uematsu (2015) 'Fatigue behavior of friction stir welded Al–Mg–Sc alloy' *International Journal of Fatigue*, Vol.77, pp.1-11